Metabolic and demographic evolution in response to interspecific competition

Authors: Giulia Ghedini[1,2]*, Dustin J. Marshall[1]

Affiliations:

[1] Centre for Geometric Biology, School of Biological Sciences, Monash University; Clayton campus, 3800 Clayton, VIC, Australia.

[2] Present address: Instituto Gulbenkian de Ciência; Rua Quinta Grande 6, 2780-156 Oeiras, Portugal.

* Corresponding author. Email: gghedini@igc.gulbenkian.pt

Summary

Species traits can evolve rapidly in response to competition, influencing the diversity and productivity of communities. Metabolic and life history theories both predict how competition should affect metabolism, size, and demography. However, these predictions are based on indirect evidence from macroevolutionary patterns or among-species comparisons. Direct experimental tests are rare and mostly focused on single or pairs of species, so how species evolve in communities is unclear, particularly in eukaryotes. We use experimental evolution of eukaryotic marine phytoplankton to examine how metabolism, size, and demography coevolve under competition. Specifically, we compare the traits of a focal species that evolved either alone, with intraspecific competitors or with a community at two points in time. We find that the focal species evolved both size and metabolism under competition, which led to an increase in carrying capacity as in max. population density. These demographic changes were predicted by classic metabolic theory based on the species-specific scaling of metabolism with size. However, we also find important departures from theory. Evolution led to Pareto improvements in both population growth rate and carrying capacity, so the existence of classic r-K trade-offs seems less inevitable than what suggested by among-species comparisons. The finding that both intra- and inter-specific competition maximize carrying capacity through changes in size and metabolism could have important consequences for our ability to predict evolution in communities.

Keywords: energy flux, community, species interactions, fitness, homeostasis, resources

Introduction

When ecological and evolutionary processes occur on similar timescales, eco-evolutionary dynamics can shape the diversity and functioning of communities (1–3). Studies in bacteria imply that competition from whole communities influences evolution in ways that are fundamentally different from simpler pairwise interactions (4–6). Whether these results extend to eukaryotic communities, where species have lower population densities and longer life cycles, remains unclear (7). Macroevolutionary patterns suggest that competition for resources should drive species to evolve different traits (e.g. Darwin's finches) (8–10). Divergence in resource-exploiting traits should reduce the intensity of competition because it minimizes overlap between species. However, when species compete for non-substitutable resources, trait divergence might not be a viable option to escape competition – which has been shown both theoretically (11,12) and empirically (3,13,14). Resolving the eco-evolutionary mechanisms that maintain the diversity of such communities remains a formidable challenge (15).

Metabolic theory has long proposed that metabolism should alter competition by setting *per capita* resource demands (16,17). For example, because of their lower absolute metabolic rates, smaller organisms have higher maximum population densities than larger organisms (18). Similarly, because small organisms usually have higher metabolism per unit mass, their populations should grow faster than those of larger organisms but sustain lower total biomass (17). Therefore, changes in size and metabolism should both affect a population's demography (19,20) but these predictions are derived from among-species comparisons that might not reflect how size, metabolism and demography covary within species (21,22). Furthermore, metabolic theory centres on the special case that resource acquisition is independent of metabolic rate, which is likely violated in many populations (23,24). If resource acquisition positively covaries with metabolism, competition could favour the evolution of larger sizes, as predicted by classic r-K models (25), but these ideas have never been tested in communities.

We combined experimental evolution and metabolic theory to determine how size, energy fluxes, and demography coevolve in response to competition. We base our assessment on a focal species, the marine eukaryotic microalga *Dunaliella tertiolecta*, which we evolved for 10 weeks in one of three competitive environments. To manipulate competition we used dialysis bags that physically isolated the focal species from its competitors while maintaining competition for light and nutrients (6,26–28).

66 The environments were: 1) the species surrounded by no competitors, 2) intraspecific competitors (a
67 population of the same species) or 3) interspecific competitors (a community of three other
68 phytoplankton species) (Fig. 1). We take the population not surrounded by competitors as a reference
69 control. Each week we batch-transferred both the focal species and the competitors, standardizing
70 biovolumes between treatments. At two points in time (after 5 and 10 weeks) we used common
71 garden experiments to determine how the life history traits of the focal species evolved: metabolism
72 (photosynthesis, respiration, and net daily energy production), morphology (cell size and shape) and
73 demography (growth rate, max. population density, and max. total biomass).

74

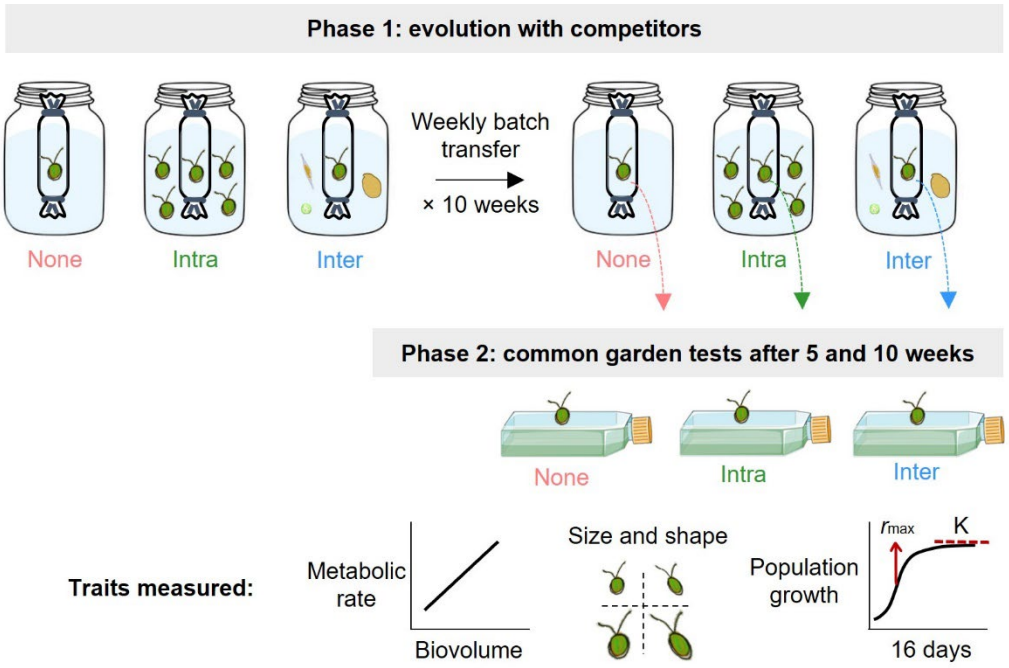

75

76 **Figure 1.** Experimental design. The focal species *Dunaliella tertiolecta* was grown in a dialysis tubing
77 placed in one of 3 environments for 10 weeks: with no competitiors ("none"), with intraspecific
78 competitors ("intra") or with a community of three interspecific competitors ("inter"). Each week we
79 performed a batch transfer of both the focal species and competitors. Mid-way (after 5 weeks) and at
80 the end of this experiment (10 weeks) we quantified changes in metabolism (photosynthesis,
81 respiration), morphology (size, shape), demography (r_{max}, K_{cells}, K_{bio}) of the focal species in common
82 garden experiments.

83

Results

Metabolism evolves under competition but the effects depend on growth phase

Energy fluxes only showed some signs of evolution after 5 weeks of competition. We could find no differences in energy fluxes when populations were growing (photosynthesis: $F_{2,178} = 1.11$, $p = 0.33$; respiration: $F_{2,176} = 2.75$, $p = 0.067$; Fig. S1), but when they were at stationary phase and resource limited, we found differences. Lineages exposed to interspecific competitors had generally lower rates of photosynthesis and respiration than lineages exposed to intraspecific or no competitors (photosynthesis: competition × biovolume interaction, $F_{2,270} = 3.85$, $p = 0.02$; respiration: main competition effect, $F_{2,272} = 6.56$, $p = 0.002$; Fig. S1, Table S1).

We observed stronger, more consistent signatures of metabolic evolution after 10 weeks in the different competition regimes. During the growth phase, competition increased photosynthesis but this positive effect weakened as biovolume increased (competition × biovolume: $F_{2,210} = 3.59$, $p = 0.03$); while the intra- and inter-specific treatments were almost overlapping, only intra- and no competition had a significant difference in slope (Fig. 2a, Table S1). Competition also affected respiration and the evolved response was consistent across biovolumes (competition effect: $F_{2,46} = 10.86$, $p < 0.001$): lineages exposed to interspecific competitors evolved to have higher metabolism (Fig. 2c, Table S1).

During the stationary phase, the patterns in evolved metabolic responses were quite different. Lineages exposed to interspecific competitors had lower photosynthesis rates than either the intra- or no competition lineages (competition effect: $F_{2,47} = 6.75$, $P = 0.003$; Fig. 2b, Table S1). We found the same for respiration – lineages exposed to interspecific competition had evolved much lower respiration rates ($F_{2,47} = 15.83$, $p < 0.0001$, Fig. 2d, Table S1).

We found very similar patterns when we estimated net energy production from photosynthesis and respiration rates on a daily cycle. When populations were growing, lineages exposed to competition produced more net energy but this declined as biovolume increased (Fig. 2e). When populations approached carrying capacity, the lineages exposed to interspecific competitors had much lower rates of net energy production (Fig. 2f).

At this point in time (10 weeks), we calculated the scaling of metabolism with cell size for our species for the three competition treatments together. We found that both photosynthesis and respiration rates scaled hyper-allometrically with cell size (P: 1.31 [CI: 1.05; 1.58]; R: 1.28 [1.02; 1.55]) but the scaling

113 became progressively shallower as populations grew denser over time (–0.06 and –0.05 per day,
114 respectively). Results did not qualitatively change when we analysed each competition treatment
115 separately, as each of them scaled > 1 and declined over time (Table S2).

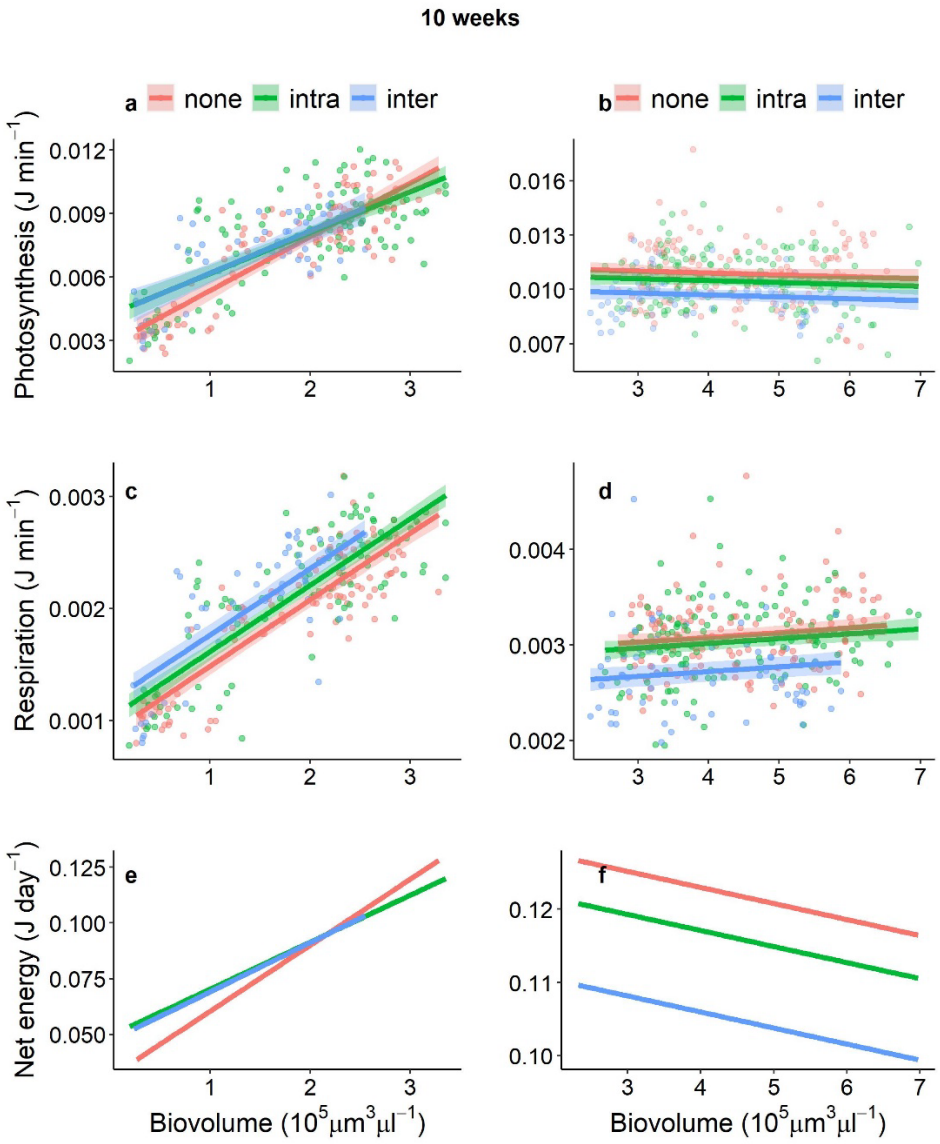

116

117 **Figure 2.** Oxygen evolution rates during the exponential growth phase (left) and stationary phase
118 (right) after ten weeks with competitors. Populations exposed to competitors evolved greater
119 photosynthesis (a) and respiration rates (c) during the growth phase. When approaching carrying
120 capacity, populations that experienced competition from interspecifics evolved much lower metabolic
121 rates (b for photosynthesis, d for respiration). Estimates of daily net energy production follow similar
122 patterns (e and f).

123 *Competition alters the morphology of cells*

124 Competition induced evolutionary changes in the size and shape of cells, which were visible despite
125 variations in both size and shape as populations grew during common gardens (time × competition,
126 Table S3, Fig. S2). Cells exposed to competition evolved smaller sizes than no-competition cells (Fig.
127 3a for day 3 after 10 weeks). There was no difference in cell size between intra- and inter-specific
128 competition after 5 weeks (Table S4), but after 10 weeks cells experiencing interspecific competition
129 were the smallest (no competition > intra > inter; Fig. 3a; Table S4 for post hoc comparisons for each
130 day). Shape evolved with size as the smaller cells exposed to competitors were also rounder (Fig. 3b
131 for day 3; Fig. S2 for all days; Table S4 for post-hoc comparisons).

132

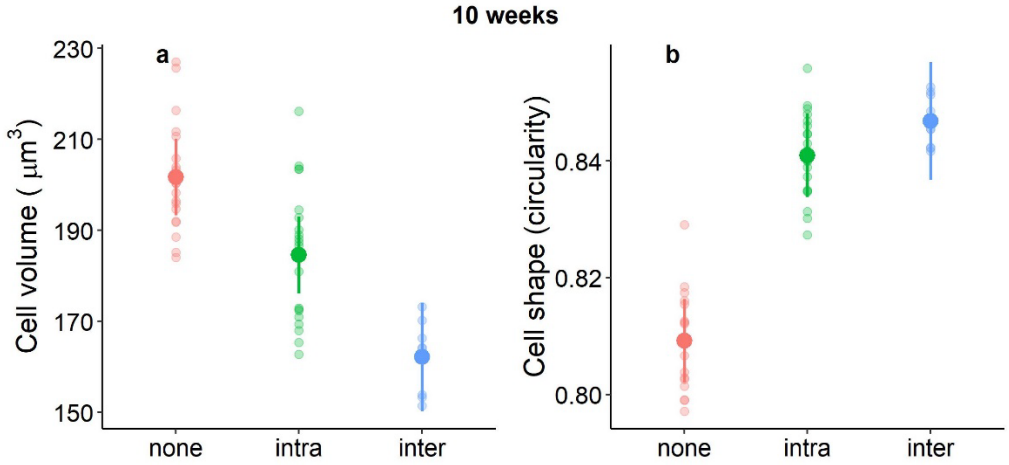

133

134 **Figure 3.** Both cell size and shape evolve in response to competition. After 10 weeks, lineages
135 exposed to competitors evolved smaller cell sizes and this decline is stronger in response to
136 interspecific competitors (a, here shown for day 3). Changes in cell size are accompanied by changes
137 in shape: the smaller cells exposed to competitors are rounder than cells that experienced no
138 competition; we find no effect of the type of competitors on shape (intra = inter). See Fig. S2 for the
139 complete temporal series.

Demography evolves to maximise maximum population density

Our focal species evolved its demography in response to competition. After 5 weeks, lineages that experienced competition had lower maximum growth rates but greater carrying capacity than lineages grown without competitors, displaying the classic trade-off between r and K in terms of cell numbers (effect of competition on r_{max}: $F_{2,42} = 10.46$, $p < 0.0005$, Fig. 4a; effect on K_{cells}: $F_{2,42} = 19.18$, $p < 0.001$, Fig. 4b). The evolved demographic responses were similar regardless of whether competition was intra- or inter-specific (Fig. S3, Table S5). After 10 weeks, we found the same evolved difference in carrying capacity (K_{cells}; $F_{2,46} = 13.91$, $p < 0.001$, Fig. 4d) but the competition-exposed lineages had evolved max. growth rates that were equivalent to the competition-free lineages ($F_{2,46} = 1.97$, $p = 0.15$, Fig. 4c; Table S5).

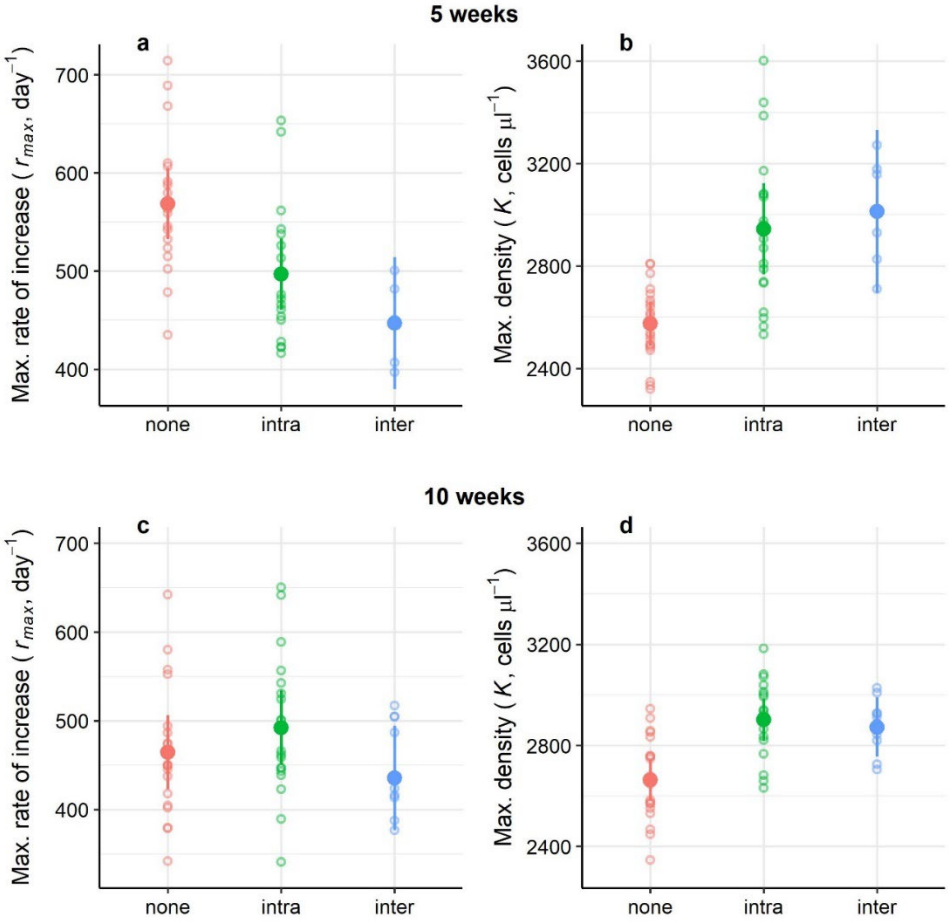

Figure 4. Populations that previously experienced competition had lower maximum population growth rates but greater carrying capacity in terms of cell numbers after 5 weeks (top row). Differences in carrying capacity persisted after 10 weeks but with no difference in growth rates (bottom row). At either time, the type of competition experienced (intra- or inter-specific) did not affect population growth parameters.

Does the scaling of metabolism with size explain demographic changes?

We used the scaling of respiration with cell size for any given day for our species (estimated above, see "*Metabolism*") to determine the expected scaling of max. growth rate (r_{max}), max. population density (K_{cells}) and total biomass at carrying capacity (K_{bio}) according to classic metabolic theory. Both metabolic scaling and demographic parameters are those measured after 10 weeks of evolution.

The theory assumes that the cost of production is directly proportional to cell size (scales with size at 1) (17,21). Therefore, demographic parameters should scale at:

(1) $r_{max} = M^B/M^1 = M^{B-1}$

(2) $K_{cells} = M^0/M^B = M^{-B}$

(3) $K_{bio} = M \times K_{cells} = M \times M^{-B} = M^{1-B}$

We used early (days 1-5) respiratory scaling values for expectations about r_{max} because it is mostly determined by growth rates early on. We used late (days 12-16) respiratory scaling values for expectations about K_{cells} and K_{bio} because cultures reached carrying capacity in the later part of the common garden and because cell size (which affects estimates of K_{bio}) stabilised around day 12 (Fig. S2). Based on these predictions, we expect that r_{max} scales positively with cell size ($B - 1 = 0.13$) and K_{cells} scales negatively ($-B = -0.59$), so that larger cells should have greater population growth and lower carrying capacities in terms of max. cell densities. We also expect that K_{bio} scales positive with size ($1 - B = 0.40$) so that large cells sustain greater max. total biomass.

We then determined the empirical scaling of each demographic parameter with cell size for our populations, using the average cell size calculated over the same intervals above (i.e., over the first five days for r_{max}, between day 12 and 16 for K_{cells} and K_{bio}). We find that our data overall align with predictions from theory. We find a weaker relationship than predicted between r_{max} and size (0.06 instead of 0.13); this relationship is non-significant as the confidence intervals overlap zero ($F_{1,48} = 0.02$, $p = 0.88$; CI: –0.71; 0.83; Fig. 5a). In quantitative agreement with theory, we find that K_{cells} declines (–0.56 instead of –0.59; $F_{1,48} = 22.4$, $p < 0.001$; CI: –0.79; –0.32; Fig. 5b), while K_{bio} increases with size (0.44 instead of 0.40; $F_{1,48} = 14.1$, $p < 0.001$; Fig. 5c).

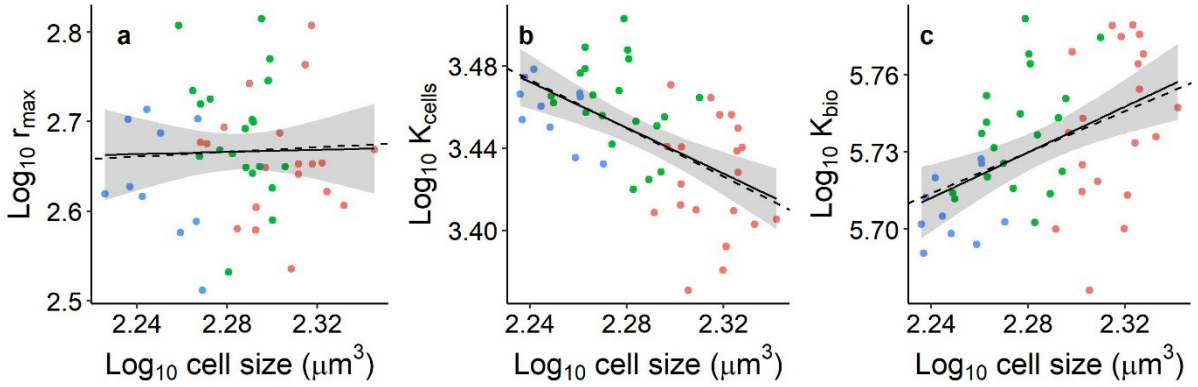

Figure 5. Scaling of max. growth rate (r_{max}), max. cell density (K_{cells}) and max. biovolume (K_{bio}) with cell size observed from our data after 10 weeks with competitors (solid line) and predicted from classic metabolic theory (i.e. assuming that the cost of production scales with size at 1; broken line). Slopes are: r_{max} = observed 0.06 (CI: –0.71; 0.83); expected 0.13; K_{cells} = observed –0.56 (CI: –0.79; –0.32); expected –0.59; K_{bio} = observed 0.44 (CI: 0.21; 0.68); expected 0.40. Scaling exponents are calculated for the 3 competition treatments together (blue = inter; green = intra; red = no competition). We calculated the expected scaling of r_{max} as the average scaling observed over the first 5 days because growth is determined early on; we calculated the expected scaling of K_{cells} and K_{bio} as the average scaling over the last 3 sampling days (12 to 16) because the cultures approached K towards the end of the common garden and cell size stabilised from day 12 onwards (Fig. S2). We used the same range of days to calculate the average cell size for each replicate shown above.

Discussion

A eukaryote evolved its size and metabolism to alter its demography and better tolerate interspecific competition. Our focal lineages first evolved higher carrying capacities in terms of population densities at the expense of faster population growth rates. But, through metabolic and size evolution, they later achieved a Pareto improvement maximising both growth rates and carrying capacity via more efficient resource use. We show that these changes in demography are predicted by classic metabolic theory, based on the scaling of metabolism with size for our species, and assuming that the cost of producing a new organism is directly proportional to its size (16,19). Accordingly, competition from a community led to the evolution of smaller cells that sustained greater maximum population densities but lower total biomass, similarly to the patterns observed among species (29).

Our results extend the main prediction of life history theory to interspecific competition from a community – competition in a stable environment tends to maximize max. population size, essentially the efficiency with which resources are converted into offspring (Table 1) (30–32). However,

increased efficiency does not necessarily come at the expense of growth rate, contrary to expectations based on classic metabolic (17,33) or life history theories (25,34–36). Empirical evidence for the existence of trade-offs within species is scarce and mostly indirect. Trade-ups seem actually more common than trade-offs; for instance, phytoplankton can improve competitive ability for different resources at no detectable cost (14,15) and bacteria can evolve larger cells that also grow faster than smaller cells despite their hypo-allometric metabolic scaling (21). We show that competition-induced evolution can break a fundamental assumption of life history theory based on r-K selection models (31,32,37). So trade-offs between r and K are not as inevitable as it has been supposed, potentially because the concomitant evolution of size and metabolism reduces constraints on production (21,38).

Metabolism fuels biological production (growth) and therefore should be under selection with intense competition (39). Among-species comparisons suggest that selection for efficiency should be associated with larger body sizes and lower metabolic rates (16,25,40). We find that this prediction does not hold for our species because it is based on general assumptions of how metabolism scales with size across species, i.e. hypo-allometrically. Our species showed hyper-allometric scaling of both photosynthesis (1.31) and respiration (1.28) with cell size. So, while larger cells produced more energy, they were also more expensive to maintain. Accordingly, populations exposed to competitors evolved smaller sizes which are more energetically advantageous under intense resource competition. These smaller cells had similar growth rates but greater max. cell density than larger cells, in qualitative and quantitative agreement with predictions from metabolic theory (i.e., assuming that the cost of production scales at 1). So it seems that metabolic theory can predict how changes in size and metabolism affect key demographic parameters within species, when using context-specific scaling rather than across species relationships.

That the scaling of metabolism with body size varies among species and environmental conditions is now well accepted (41). However, there is less recognition for the role of plasticity in metabolic scaling within the same population, even though it is important to maintain fitness and energy homeostasis (42,43). Competition should drive the evolution of fitness-enhancing metabolic traits, but both fast and slow metabolic phenotypes have been proposed to be a product of competition. A slow metabolism can be advantageous when resources are limited (24) but can come at the expense of competitive ability (44) and access to resources (23). Our results show that fluctuations in population densities

239 can maintain both metabolic phenotypes even under strong competition. All our experimental
240 populations reduced their metabolism during the stationary phase, which seems to be common
241 among many phytoplankton species to cope with nutrient limitation (45). But this metabolic flexibility
242 was heightened by competition, so that populations with a history of competition had a faster
243 metabolism when resources were abundant but much lower metabolic rates when population were
244 dense.

245 In our species, competition selected for efficiency by favouring small cells with a lower metabolic rate
246 per unit volume when resources were scarce (because of their hyper-allometric metabolic scaling).
247 The advantage of small cells under nutrient limitation is well established among phytoplankton
248 species (46); here we show that these across-species patterns might also hold within species.
249 Smaller cells have several advantages that enables them to produce more cells per unit nutrient
250 (38,47). They have lower sinking rates, hence more access to light, suffer less from self-shading, and
251 are more efficient in the acquisition of nutrients due to a higher surface to volume ratio (48,49). While
252 changes in shape can reduce the constraints of larger cell sizes on nutrient acquisition (48,50), we
253 find that competition favours the evolution of smaller cells, rather than cells of similar size but different
254 shape. However, overall, size and shape covaried as predicted because small, evolved cells were
255 rounder than the larger cells not exposed to competitors.

256 Predicting how species evolve in communities remains a formidable challenge (51–53). Interactions
257 among multiple species can diffuse competition (54), weakening selection between any pair of
258 competitors (55,56). Our results show that both intra- and inter-specific competition from a community
259 select for efficiency (carrying capacity of individuals), which is achieved through the concomitant
260 evolution of size and metabolism. Overall, competition from a community exerted stronger effects on
261 the evolution of these traits than intraspecific competition, possibly because diverse competitors
262 consume available resources more rapidly and effectively (57,58). But it seems that the classic
263 prediction of life history theory (selection for K under density-dependence (31)) can be extended to
264 competition in communities, at least for species that use essential resources. Finding whether
265 interspecific competition leads to the same evolutionary outcomes in other systems seems key to
266 predict the evolutionary trajectory of species in communities. Interestingly, the traits that evolved more
267 strongly under interspecific competition (i.e. size and metabolism) are also those that affect niche and
268 fitness differences between species (59,60). Hence, a next important step would be to test how life

history optimization influences the coexistence of coadapted species through changes in their metabolic scaling. Understanding how metabolism, size, and demography covary between competing species is essential to explain patterns of biological production and extrapolate the effect of biodiversity over time (1,22).

Table 1. Predicted and observed changes in life history traits based on the history of competition. We base the main predictions on the effects of intra-specific competition and elaborate on the predicted effects of interspecific competition on the last row.

Trait	Predicted effect of intrasp. competition	Key references	Observed effect
r_{max}	Decrease in a stable or low stochastic environment with high population density	MacArthur 1962, MacArthur & Wilson 1967 Mueller et al 1991 Lande et al. 2009 Engen & Sæther 2017 Kentie et al. 2020	Yes / No (tradeoff with K weakens over time)
K_{cells} *	Increase		Yes
Size	Increase under K-selection	Pianka 1970 Bierbaum et al. 1989	No
	Decrease based on effects of nutrient limitation on phytoplankton	Litchman & Klausmier 2008	Yes
Shape	More elongated to reduce surface area to volume ratio and improve nutrient uptake if cells become larger	Grant et al. 2021 Ryabov et al. 2021	No (larger cells were more elongated but were not those exposed to competitors)
	Rounder if cells become smaller		Yes
Metabolism	Lower metabolism, increased efficiency under K-selection	Pianka 1970, 1972 Mueller & Diamond 2001 Lenski 2003 Auer et al. 2018	Yes closer to carrying capacity
	Increased metabolic rate (faster pace of life) but only if resources are abundant	Auer et al. 2020 Pettersen et al. 2020	Yes during growth phase
Effect of interspecific competitition	If resource overlap among species is significant, interspecific competition should strengthen density-dependence and thus the K-selection observed under intraspecific competition alone.	MacArthur & Wilson 1967 Bassar et al. 2013 Lawrence et al. 2012 Jousset et al. 2016 Scheuerl et al. 2020	Yes for size and metabolism. No for r_{max}, K_{cells}, and cell shape

* Opposite pattern if the environment is highly stochastic and/or with low density-dependence (r_{max} increases and K_{cells} decreases). We do not expect this scenario because our environent is not highly stochastic and our populations density-regulated.

Materials and Methods

Overview of experimental set up

We tested the effects of competition on the energy fluxes, morphology, and demography of the eukaryotic unicellular alga *Dunaliella tertiolecta*, which we obtained as a clonal strain from the CSIRO Australian National Algae Culture Collection (ANACC, strain CS-14). To manipulate the competitive environment, we enclosed the focal species in a dialysis bag which was then place in one of three environments for 10 weeks (1st June to 10th August 2021): 1) surrounded by media with no competitors (no competition), 2) by a population of conspecifics from the same strain (intraspecific competition) or 3) by a community of three other phytoplankton species (interspecific competition). For this latter treatment, the species were chosen to represent different sizes and phytoplankton groups: *Amphidinium carterae* (CS-740), *Phaeodactylum tricornutum* (CS-29) and *Nannochloropsis oculata* (CS-179) (Fig. 1, phase 1). All species were sourced as clonal strains from CSIRO Algal collection. Every week we batch-transferred both the focal species and the competitors. After 5 and 10 weeks, we quantified changes in the traits of the focal species in common garden experiments (phase 2).

We grew all species individually in 2 L glass bottles with standard f/2 enriched seawater medium enriched with silica for a month prior to the experiment. The same medium was used throughout the experiment and common gardens. The medium was prepared with 0.45 µm filtered seawater and autoclaved following the recipe of Guillard & Ryther, 1962 (61). All experiments were performed in a temperature controlled room (20 ± 1°C) on a 14:10 hours light:dark cycle and the cultures were grown under a light intensity of 115 ± 5 µmol photons m^{-2} s^{-1}.

Phase 1: evolution with competitors

The dialysis bags in which we enclosed the focal species enabled competition for light and nutrients but prevented cell mixing among phytoplankton species and exchange of bacteria (pore diameter = 24 Angstrom). Each bag contained a volume of 35 ml and was placed at the centre of a 500 ml glass jar assigned to one of the three competition treatments above. We established 20 replicates for each competition treatment. We quantified the biovolume of each species as the product of cell density and cell size. For each species, we loaded two 10 µl samples onto a Neubauer counting chamber (ProSciTech, Australia), fixed with 1% lugol's solution, and, for each sample, we took 20 photos

equally spaced around the cell counting grid under an Olympus light microscope at 400× magnification. We analysed the images with ImageJ and Fiji software (version 2.0) (62) to quantify the number of cells (cells μl^{-1}) and their size (µm, length and width; diameter for *Nannochloropsis*). We calculated cell volume by assigning to each species an approximate geometric shape (63) (prolate spheroid $V = (pi/6) \times width^2 \times length$ for all species except *Nannochloropsis* which we treated as a sphere $V = (pi/6) \times diameter^3$). Cell circularity is calculated as $4 \times pi \times (area/perimeter^2)$ and ranges from 0 to 1 (perfect circle).

We started the experiment with an initial biovolume of 9.6×10^8 μm^3 of the focal species which corresponded to 5 ml. The dialysis bag was then filled to 35 ml with media. The glass jars containing the competitors were filled to 350 ml to completely submerge the dialysis bag. To maintain the same biovolume to media ratio, the initial biovolume of the competitors was 10 times that of the focal species (i.e. 9.6×10^9 μm^3). We added the three competitor species of the interspecific treatment in equal biovolumes. The jars of the control treatment (no competition) were filled with medium only.

Each week we transferred the same initial biovolume of the focal species and the same initial biovolume of the competitors to a new, sterilized set of dialysis bag and jar. We did not manipulate the relative abundance of species in the interspecific treatment. In weeks 3, 5 and 6 the cell densities of the focal species were low in the interspecific treatment. So, had we reinoculated the same initial biovolume we would not have been able to add any fresh medium. To avoid this nutrient limitation, we reinoculated only half of the initial biovolumes across all treatments. Cell densities, size and biovolume were determined as described above. By week 6, we discarded 13 lineages of the focal species in the interspecific treatment because they were contaminated by the diatom. To continue the experiment, we established an additional lineage from each of the remaining seven replicates. By the end of the experiment, we lost 4 other replicates in the interspecific treatment because of contamination.

The batch-transfer approach meant that all populations in our experiment experienced fluctuating densities, but those surrounded by competitors always faced greater densities and thus competition. Shifts in densities are common in nature and mediate the balance between density-independent and density-dependent selection (r- and K-selection) (37). If stochasticity is low, theory predicts that selection for K should prevail even under fluctuating conditions (Table 1) (25,31,64).

Phase 2: common garden experiments

To test the effects of competition on the metabolism, morphology, and demography of the focal species we did two common garden tests, one after five weeks of evolution with competitors (samples were taken at the start of week six, 6th July 2021) and one after ten weeks (10th August, end of experiment). Before each common garden, we grew the focal species in a neutral environment for two nights to remove any environmental conditioning. Both for the neutral selection and common garden, we inoculated an equal biovolume of each lineage in cell culture flasks (n = 20 for the no competition and intraspecific treatments, n = 6 and n = 10 for the interspecific treatment in the first and second common garden, respectively). Biovolume was determined as before from the average cell size and cell density of each lineage; we decided a priori to add 15 ml of the lineage with the limiting biovolume (~14 × 10^8 μm^3), back calculated the volumes of the other lineages and added 100 ml of f/2 media plus silica to all flasks. Common gardens started on 8th July and 12th August 2021 and lasted 16 days which was the approximate time needed for the cultures to reach carrying capacity. Each day, we removed 10 ml from each culture flask for sampling and replaced it with fresh media. In the first common garden we sampled every day except on day 6, 10, 13 and 15; in the second we sampled every day except on day 7, 13 and 15.

Traits measurements

Each sampling day, we fixed 1 ml sample with 1% Lugol's solution to quantify the cell size (volume), shape (circularity) and abundance of each lineage with ImageJ software as described above. We include cell shape in addition to size in our assessment because the shape of a cell can mediate access to resources and is thus an important component of fitness in unicellular organisms (48–50,65).

We measured oxygen evolution rates on 5 ml samples using 24-channel optical fluorescence oxygen readers (PreSens Sensor Dish Reader, SDR; AS-1 Scientific Wellington, New Zealand) following established protocols (66,67). Sensors were calibrated with 0% and 100% air saturation before the experiment. Net photosynthesis (oxygen production) was measured at the same light intensity at which the cultures were grown for 20 minutes, followed by 1 hr in the dark to measure respiration rates. Thirteen blanks were filled with the media obtained from centrifuged samples (spun at 2,500 rpm for 10 min to separate the algae from the supernatant) to correct for background microbial activity

since cultures were not axenic. Prior to measurements, samples were spiked with 50 µl of sodium bicarbonate stock for a final concentration of 2 mM sodium bicarbonate to avoid carbon limitation.

The change in percentage oxygen saturation was calculated with linear regressions using the LoLinR package (68). The rate of photosynthesis or respiration of the whole sample (VO_2; units µmol O_2/min) was then measured as $VO_2 = 1 \times ((m_a - m_b)/100 \times V\beta O_2)$ following (69), where m_a is the rate of change of O_2 saturation in each sample (min^{-1}), m_b is the mean O_2 saturation across all blanks (min^{-1}), V is the sample volume (0.005 L) and $V\beta O_2$ is the oxygen capacity of air-saturated seawater at 20°C and 35 ppt salinity (225 µmol O_2/L). The first 3 minutes of measurements in the light were discarded for all samples. Respiration rates were calculated after 15 minutes of dark when oxygen levels showed a linear decline. Photosynthesis and respiration (µmol O_2/min) were converted to calorific energy (J/min) using the conversion factor of 0.512 J/µmol O_2 to estimate energy production and energy consumption respectively (70).

Statistical analyses

All analyses and plots were done in RStudio (version 4.1.3), separately for the two common gardens.

Morphology. We assessed differences in cell morphology (cell size or shape) with linear mixed models including competition treatment (3 levels) and time (day) as categorical predictors, and lineage identity as random intercept to account for repeated measures; time was considered categorical because the relationship with cell morphology was non-linear. We take day 3, during the exponential growth phase, as a reference to report post hoc results on differences in cell size and shape, and we report post hoc results for each day in supplements.

Demography. To test differences in the maximum rates of increase (r_{max}) and maximum values (K_{cells}) of cell density we followed a three-step approach (described in detail in Ghedini et al. 2021 (67), adapted from Malerba et al., 2018 (71)). First, we fitted four growth models to each individual replicate lineage and chose the best-fitting model among the four candidates to best describe changes in the cell density (cells/µl) of each culture over time. We used AIC to determine which growth model best described the dynamics of a culture and successful convergence was ensured for all best-fitting models. The four models were: a logistic-type sinusoidal growth model with lower asymptote forced to 0 (i.e. three-parameter logistic curve), a logistic-type sinusoidal growth model with non-zero lower asymptote (i.e. four-parameter logistic curve), a Gompertz-type sinusoidal growth model (i.e. three-

parameter Gompertz curve) and a modified Gompertz-type sinusoidal growth model including population decline after reaching a maximum (i.e. four-parameter Gompertz-like curve including mortality). Second, we used the best-fitting model to estimate growth parameters (i.e. r_{max} and K) for each culture. From each nonlinear curve, we extracted the maximum predicted value (K) of population density (cells μl^{-1}). From the first derivative of the curve, we extracted the maximum rate of population increase (r_{max}, unit: day^{-1}). Third, we used an analysis of covariance to evaluate the influence of competition on each parameter, using a linear model including the initial cell density estimated from the previous step as a covariate and competition environment as a factor (three levels). The estimates of K of the first common garden had heterogeneous variances among treatments, so we used generalized least squares models (instead of linear models) including treatment-specific variance for each level of competition treatment (varIdent function in R). We then estimated and plotted least square means and 95% confidence intervals using Tukey p-value adjustment for comparing three estimates. Finally, we fitted the same nonlinear growth models described above across all lineages within each competition treatment to visualize qualitative differences in population growth, using AIC to select the best-fitting model.

Metabolism. While oxygen rates increased linearly with biovolume over the first few days, this relationship broke down in the second part of the common garden as biovolume increased (> ~3 $\mu m^3/\mu l$) (Fig. S4). Log-transformation did not result in linearity across the entire range of biovolume. Therefore, we analysed oxygen rates separately for the first part of the common garden during the exponential growth phase (from the day after inoculation to day 6 included), and for the second part during the stationary phase (day 7 to 16). We used linear mixed models including biovolume (covariate) and competition treatment as predictors and lineage identity as random intercept for the data of the second common garden. Because variances were heterogenous for the photosynthesis data during the growth phase we used a generalised linear mixed model including competition-specific variances. As a last step, we estimated and plotted the net energy production of the whole sample over a 24-hr period (J/day) as 14 hr of energy produced through net photosynthesis minus 10 hr of respiration using the predictions from the models.

We could not use mixed models on the oxygen evolution data from the first common garden because of a singular fit error likely due to the lower replication of the interspecific competition treatment (n = 6). Therefore, we used linear models with biovolume (covariate) and competition treatment as

predictors (i.e. without including lineage identity). While this is not ideal, we repeated the analyses for the August data with simple linear models and obtained the same results of mixed models (results not reported here), suggesting that oxygen rates are not strongly affected by lineage identity. Nonetheless, we report the results on oxygen rates for the first common garden as a supplementary figure. For all analyses of oxygen rates, data were not transformed but biovolume was rescaled to 10^{-5} μm^3 μl^{-1}. Interactions between biovolume and competition were removed when $p > 0.25$ or if the interaction was not significant and the model with interaction did not perform better than the simpler model compared by AIC and anova.

Scaling of demographic parameters with cell size. First, we determined the scaling of metabolism with cell size for our evolved populations after ten weeks of evolution. For this assessment we combined the data of the three competition treatments which allowed us to assess a wider range of sizes. We calculated the scaling of respiration and photosynthesis, separately, from linear models including cell size and experiment day as numerical predictors. Oxygen rates and cell size were $\log_{10}$-transformed. We also calculated the scaling of metabolic rates with size for each competition treatment individually and obtained the same qualitative results (Table S2 in supplements). Based on these results (effects of size and experiment day), we then calculated the expected scaling of respiration with size for any given day. According to classic metabolic theory, the cost of production is directly proportional to cell size (scales with size at 1) (17,21), so demographic parameters should scale with size at:

(1) $r_{max} = M^B/M^1 = M^{B-1}$

(2) $K_{cells} = M^0/M^B = M^{-B}$

(3) $K_{bio} = M \times K_{cells} = M \times M^{-B} = M^{1-B}$

We used early (days 1-5) respiratory scaling values for expectations about r_{max} because it is mostly determined by growth rates early on. We used late (days 12-16) respiratory scaling values for expectations about K_{cells} and K_{bio} because cultures reached carrying capacity in the later part of the common garden and because cell size (which affects estimates of K_{bio}) stabilised around day 12. We estimated maximum total biomass (K_{bio}) as the product of K_{cells} obtained from the population growth models and the average cell size for each replicate over the last three sampling days (day 12 to 16), that is when cell size stabilised. Finally, we determined the empirical scaling of each demographic parameter with cell size across our populations, using the average cell size calculated over the same intervals above (i.e., over the first 5 days for r_{max}, between day 12 and 16 for K_{cells} and K_{bio}).

458

459 **Acknowledgements**

460 We thank Jiaye Qin for assistance in the laboratory. This work was supported by a DECRA fellowship
461 (DE190100660) at Monash University to GG. This work also received the support of a fellowship
462 (LCF/BQ/PI21/11830001) from "la Caixa" Foundation (ID 100010434) and from the European Union's
463 Horizon 2020 research and innovation programme under the Marie Skłodowska Curie grant
464 agreement No 847648.

465

466 **References**

467 1. Aubree F, David P, Jarne P, Loreau M, Mouquet N, Calcagno V. How community adaptation
468 affects biodiversity–ecosystem functioning relationships. Ecol Lett. 2020;23(8):1263–75.

469 2. Post DM, Palkovacs EP. Eco-evolutionary feedbacks in community and ecosystem ecology:
470 interactions between the ecological theatre and the evolutionary play. Philos Trans R Soc B Biol
471 Sci. 2009; 364:1629–1640.

472 3. Hart SP, Turcotte MM, Levine JM. Effects of rapid evolution on species coexistence. Proc Natl
473 Acad Sci. 2019;116(6):2112.

474 4. Jousset A, Eisenhauer N, Merker M, Mouquet N, Scheu S. High functional diversity stimulates
475 diversification in experimental microbial communities. Sci Adv. 2016;2(6):e1600124.

476 5. Lawrence D, Fiegna F, Behrends V, Bundy JG, Phillimore AB, Bell T, et al. Species Interactions
477 Alter Evolutionary Responses to a Novel Environment. PLOS Biol. 2012;10(5):e1001330.

478 6. Scheuerl T, Hopkins M, Nowell RW, Rivett DW, Barraclough TG, Bell T. Bacterial adaptation is
479 constrained in complex communities. Nat Commun. 2020;11(1):754.

480 7. Barraclough TG. How Do Species Interactions Affect Evolutionary Dynamics Across Whole
481 Communities? Annu Rev Ecol Evol Syst. 2015;46(1):25–48.

482 8. Grant PR, Grant BR. Evolution of Character Displacement in Darwin's Finches. Science.
483 2006;313(5784):224–6.

484 9. Rainey PB, Travisano M. Adaptive radiation in a heterogeneous environment. Nature.
485 1998;394(6688):69–72.

486 10. Schluter D. Experimental Evidence That Competition Promotes Divergence in Adaptive
487 Radiation. Science. 1994;266(5186):798–801.

488 11. Fox JW, Vasseur DA. Character Convergence under Competition for Nutritionally Essential
489 Resources. Am Nat. 2008;172(5):667–80.

490 12. Abrams PA. Character displacement and niche shift analyzed using consumer-resource models
491 of competition. Theor Popul Biol. 1986;29(1):107–60.

492 13. Germain RM, Srivastava D, Angert AL. Evolution of an inferior competitor increases resistance to
493 biological invasion. Nat Ecol Evol. 2020; 4:419–425.

14. Bernhardt JR, Kratina P, Pereira AL, Tamminen M, Thomas MK, Narwani A. The evolution of competitive ability for essential resources. Philos Trans R Soc B Biol Sci. 2020;375(1798):20190247.

15. Gallego I, Narwani A. Ecology and evolution of competitive trait variation in natural phytoplankton communities under selection. Ecol Lett. 2022; doi/abs/10.1111/ele.14103

16. Brown JH, Gillooly JF, Allen AP, Savage VM, West GB. Toward a metabolic theory of ecology. Ecology. 2004;85(7):1771–89.

17. Savage VM, Gillooly JF, Brown JH, West GB, Charnov EL. Effects of body size and temperature on population growth. Am Nat. 2004;163(3):429–41.

18. Damuth J. Population-density and body size in mammals. Nature. 1981;290(5808):699–700.

19. Isaac NJB, Carbone C, McGill B. Population and Community Ecology. In: Sibly RM, Brown JH, Kodric-Brown A, editors. Metabolic Ecology. 2012.

20. Malerba ME, Marshall DJ. Size-abundance rules? Evolution changes scaling relationships between size, metabolism and demography. Ecol Lett. 2019;22:1407–16.

21. Marshall DJ, Malerba M, Lines T, Sezmis AL, Hasan CM, Lenski RE, et al. Long-term experimental evolution decouples size and production costs in Escherichia coli. Proc Natl Acad Sci. 2022;119(21):e2200713119.

22. White CR, Alton LA, Bywater CL, Lombardi EJ, Marshall DJ. Metabolic scaling is the product of life-history optimization. Science. 2022;377(6608):834–9.

23. Schuster L, Cameron H, White CR, Marshall DJ. Metabolism drives demography in an experimental field test. Proc Natl Acad Sci U S A. 2021;118(34):e2104942118.

24. Auer SK, Bassar RD, Turek D, Anderson GJ, McKelvey S, Armstrong JD, et al. Metabolic Rate Interacts with Resource Availability to Determine Individual Variation in Microhabitat Use in the Wild. Am Nat. 2020;196(2):132–44.

25. Pianka ER. On r- and K-Selection. Am Nat. 1970;104(940):592–7.

26. Berga M, Székely AJ, Langenheder S. Effects of disturbance intensity and frequency on bacterial community composition and function. PLoS ONE. 2012;7(5):e36959–e36959.

27. Pomati F, Jokela J, Castiglioni S, Thomas MK, Nizzetto L. Water-borne pharmaceuticals reduce phenotypic diversity and response capacity of natural phytoplankton communities. PLoS ONE. 2017;12(3):e0174207.

28. Poulson-Ellestad KL, Jones CM, Roy J, Viant MR, Fernández FM, Kubanek J, et al. Metabolomics and proteomics reveal impacts of chemically mediated competition on marine plankton. Proc Natl Acad Sci. 2014;111(24):9009.

29. Hatton IA, Dobson AP, Storch D, Galbraith ED, Loreau M. Linking scaling laws across eukaryotes. Proc Natl Acad Sci. 2019;116(43):21616.

30. Charlesworth B. Selection in Density-Regulated Populations. Ecology. 1971;52(3):469–74.

31. Lande R, Engen S, Sæther BE. An evolutionary maximum principle for density-dependent population dynamics in a fluctuating environment. Philos Trans R Soc B Biol Sci. 2009;364(1523):1511–8.

32. MacArthur R. Some generalized theorems of natural selection. PNAS. 1962;48(11):1893–7.

33. Perkins DM, Perna A, Adrian R, Cermeño P, Gaedke U, Huete-Ortega M, et al. Energetic equivalence underpins the size structure of tree and phytoplankton communities. Nat Commun. 2019;10(1):255.

34. Mueller LD, Guo P, Ayala FJ. Density-Dependent Natural Selection and Trade-Offs in Life History Traits. Science. 1991;253(5018):433–5.

35. Mueller LD, Ayala FJ. Trade-off between r-selection and K-selection in Drosophila populations. Proc Natl Acad Sci. 1981;78(2):1303–5.

36. Sæther BE, Visser ME, Grøtan V, Engen S. Evidence for r- and K-selection in a wild bird population: a reciprocal link between ecology and evolution. Proc R Soc B Biol Sci. 2016;283(1829):20152411.

37. MacArthur RH, Wilson EO. The Theory of Island Biogeography. Princeton University Press; 1967.

38. Malerba ME, Palacios MM, Palacios Delgado YM, Beardall J, Marshall DJ. Cell size, photosynthesis and the package effect: an artificial selection approach. New Phytol. 2018;219(1):449–61.

39. Bassar RD, Lopez-Sepulcre A, Reznick DN, Travis J, Brodie AEED, McPeek EMA. Experimental Evidence for Density-Dependent Regulation and Selection on Trinidadian Guppy Life Histories. Am Nat. 2013;181(1):25–38.

40. Glazier DS. Is metabolic rate a universal 'pacemaker' for biological processes? Biol Rev. 2015;90(2):377–407.

41. Norin T, Metcalfe NB. Ecological and evolutionary consequences of metabolic rate plasticity in response to environmental change. Philos Trans R Soc B Biol Sci. 2019;374(1768):20180180.

42. Grant NA, Maddamsetti R, Lenski RE. Maintenance of Metabolic Plasticity despite Relaxed Selection in a Long-Term Evolution Experiment with Escherichia coli. Am Nat. 2021;198(1):93–112.

43. Auer SK, Salin K, Rudolf AM, Anderson GJ, Metcalfe NB. Flexibility in metabolic rate confers a growth advantage under changing food availability. J Anim Ecol. 2015;84(5):1405–11.

44. Pettersen AK, Hall MD, White CR, Marshall DJ. Metabolic rate, context-dependent selection, and the competition-colonization trade-off. Evol Lett. 2020;4:333–44.

45. López-Sandoval DC, Rodríguez-Ramos T, Cermeño P, Sobrino C, Marañón E. Photosynthesis and respiration in marine phytoplankton: Relationship with cell size, taxonomic affiliation, and growth phase. J Exp Mar Biol Ecol. 2014;457:151–9.

46. Litchman E, Klausmeier CA, Schofield OM, Falkowski PG. The role of functional traits and trade-offs in structuring phytoplankton communities: scaling from cellular to ecosystem level. Ecol Lett. 2007;10(12):1170–81.

47. Rabbers I, Gottstein W, Feist AM, Teusink B, Bruggeman FJ, Bachmann H. Selection for Cell Yield Does Not Reduce Overflow Metabolism in Escherichia coli. Mol Biol Evol. 2021;39(1):msab345.

48. Hillebrand H, Acevedo-Trejos E, Moorthi SD, Ryabov A, Striebel M, Thomas PK, et al. Cell size as driver and sentinel of phytoplankton community structure and functioning. Funct Ecol. 2022;36(2):276–93.

49. Litchman E, Klausmeier CA. Trait-Based Community Ecology of Phytoplankton. Annu Rev Ecol Evol Syst. 2008;39(1):615–39.

50. Grant NA, Abdel Magid A, Franklin J, Dufour Y, Lenski RE. Changes in Cell Size and Shape during 50,000 Generations of Experimental Evolution with Escherichia coli. J Bacteriol. 2021;203(10):e00469-20.

51. Barabás G, J. Michalska-Smith M, Allesina S. The Effect of Intra- and Interspecific Competition on Coexistence in Multispecies Communities. Am Nat. 2016;188(1):E1–12.

52. Levine JM, Bascompte J, Adler PB, Allesina S. Beyond pairwise mechanisms of species coexistence in complex communities. Nature. 2017; 546:56-64.

53. Yamamichi M, Gibbs T, Levine JM. Integrating eco-evolutionary dynamics and modern coexistence theory. Ecol Lett. 2022;25:2091–106.

54. Barbier M, de Mazancourt C, Loreau M, Bunin G. Fingerprints of High-Dimensional Coexistence in Complex Ecosystems. Phys Rev X. 2021;11(1):011009.

55. Miller TE, Moran ER, terHorst CP. Rethinking Niche Evolution: Experiments with Natural Communities of Protozoa in Pitcher Plants. Am Nat. 2014;184(2):277–83.

56. Lankau RA. Rapid Evolutionary Change and the Coexistence of Species. Annu Rev Ecol Evol Syst. 2011;42(1):335–54.

57. Maynard DS, Crowther TW, Bradford MA. Competitive network determines the direction of the diversity–function relationship. Proc Natl Acad Sci. 2017;114(43):11464.

58. Vallina SM, Cermeno P, Dutkiewicz S, Loreau M, Montoya JM. Phytoplankton functional diversity increases ecosystem productivity and stability. Ecol Model. 2017;361:184–96.

59. Gallego I, Venail P, Ibelings BW. Size differences predict niche and relative fitness differences between phytoplankton species but not their coexistence. ISME J. 2019;13(5):1133–43.

60. Brandl SJ, Quigley CN, Casey JM, Mercière A, Schiettekatte NMD, Norin T, et al. Metabolic rates mirror morphological and behavioral differences in two sand-dwelling coral reef gobies. Mar Ecol Prog Ser. 2022;684:79–90.

61. Guillard RRL, Ryther JH. Studies of marine planktonic diatoms. I. *Cyclotella nana* Hustedt and *Detonula confervacea* Cleve. Can J Microbiol. 1962;8:229–39.

62. Schindelin J, Arganda-Carreras I, Frise E, Kaynig V, Longair M, Pietzsch T, et al. Fiji: an open-source platform for biological-image analysis. Nat Methods. 2012;9(7):676–82.

63. Hillebrand H, Dürselen CD, Kirschtel D, Pollingher U, Zohary T. Biovolume calculation for pelagic and benthic microalgae. J Phycol. 1999;35(2):403–24.

64. Lenski RE. Phenotypic and Genomic Evolution during a 20,000-Generation Experiment with the Bacterium Escherichia coli. In: Plant Breeding Reviews. John Wiley & Sons, Ltd; 2003. p. 225–65, ch8.

65. Ryabov A, Kerimoglu O, Litchman E, Olenina I, Roselli L, Basset A, et al. Shape matters: the relationship between cell geometry and diversity in phytoplankton. Ecol Lett. 2021;24(4):847–61.

66. Malerba ME, White CR, Marshall DJ. Phytoplankton size-scaling of net-energy flux across light and biomass gradients. Ecology. 2017;98(12):3106–15.

67. Ghedini G, Marshall DJ, Loreau M. Phytoplankton diversity affects biomass and energy production differently during community development. Funct Ecol. 2022;36:446–57.

68. Olito C, White CR, Marshall DJ, Barneche DR. Estimating monotonic rates from biological data using local linear regression. J Exp Biol. 2017;220(5):759.

69. White CR, Kearney MR, Matthews PGD, Kooijman SALM, Marshall DJ. A Manipulative Test of Competing Theories for Metabolic Scaling. Am Nat. 2011;178(6):746–54.

70. Williams PJ le B, Laurens LML. Microalgae as biodiesel & biomass feedstocks: Review & analysis of the biochemistry, energetics & economics. Energy Environ Sci. 2010;3(5):554–90.

71. Malerba ME, Palacios MM, Marshall DJ. Do larger individuals cope with resource fluctuations better? An artificial selection approach. Proc R Soc B Biol Sci. 2018;285(1884):20181347.